Imperial College London

Evaluation of Hematite as a Photo-Anode

Solar Fuels Symposium
Imperial College London
13 March 2013

Dr Anna Hankin
Postdoctoral Research Associate
Electrochemical Engineering Research Group
Chemical Engineering Department

Presentation Outline

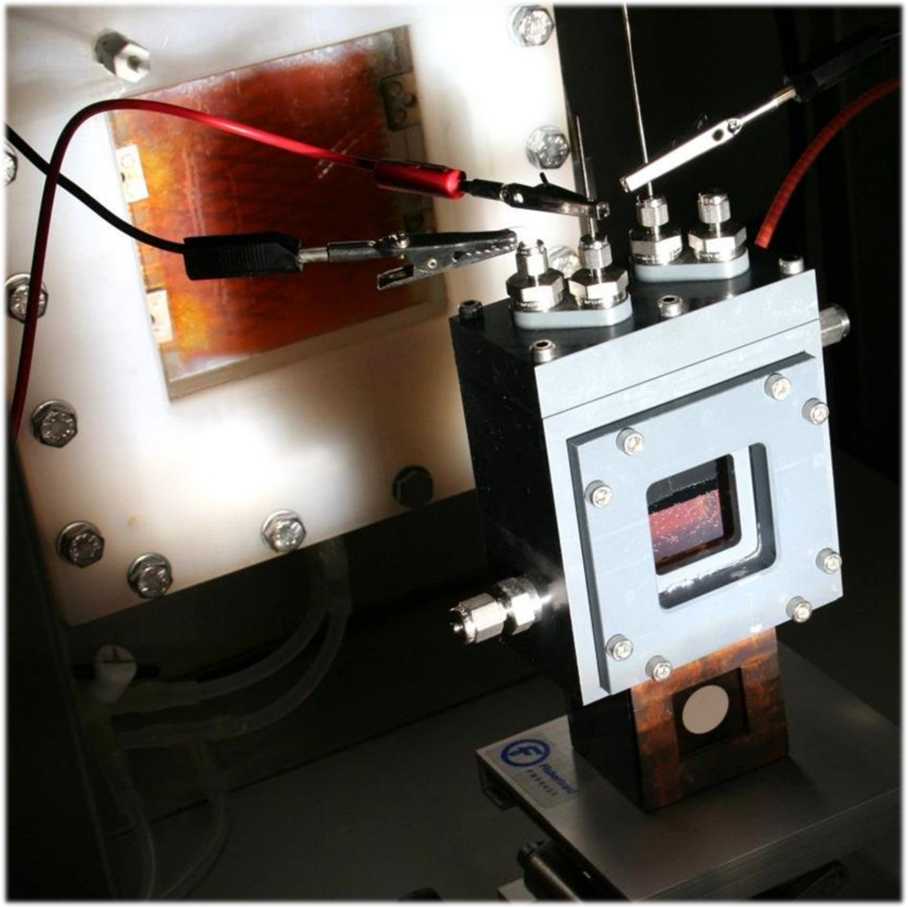

1. Theory
2. Fabrication
3. Photo-response with and without Dopants
4. Hematite | Liquid Interfacial Structure
5. Future Research

Pros and Cons of Hematite as a Photoanode

Suitability of Fe_2O_3:

- ✓ Absorption spectrum well matched to solar spectrum
- ✓ Easily fabricated on a large scale at low cost
- ✓ Stable to decomposition by ***e***$^-$ and ***h***$^+$ over wide potential range
- ✓ Valence band energy below that for decomposition of H_2O to O_2

Limitations of Fe_2O_3:

- × Conduction band energy below decomposition potential for H_2O to H_2
- × Stable only in neutral / alkaline pH

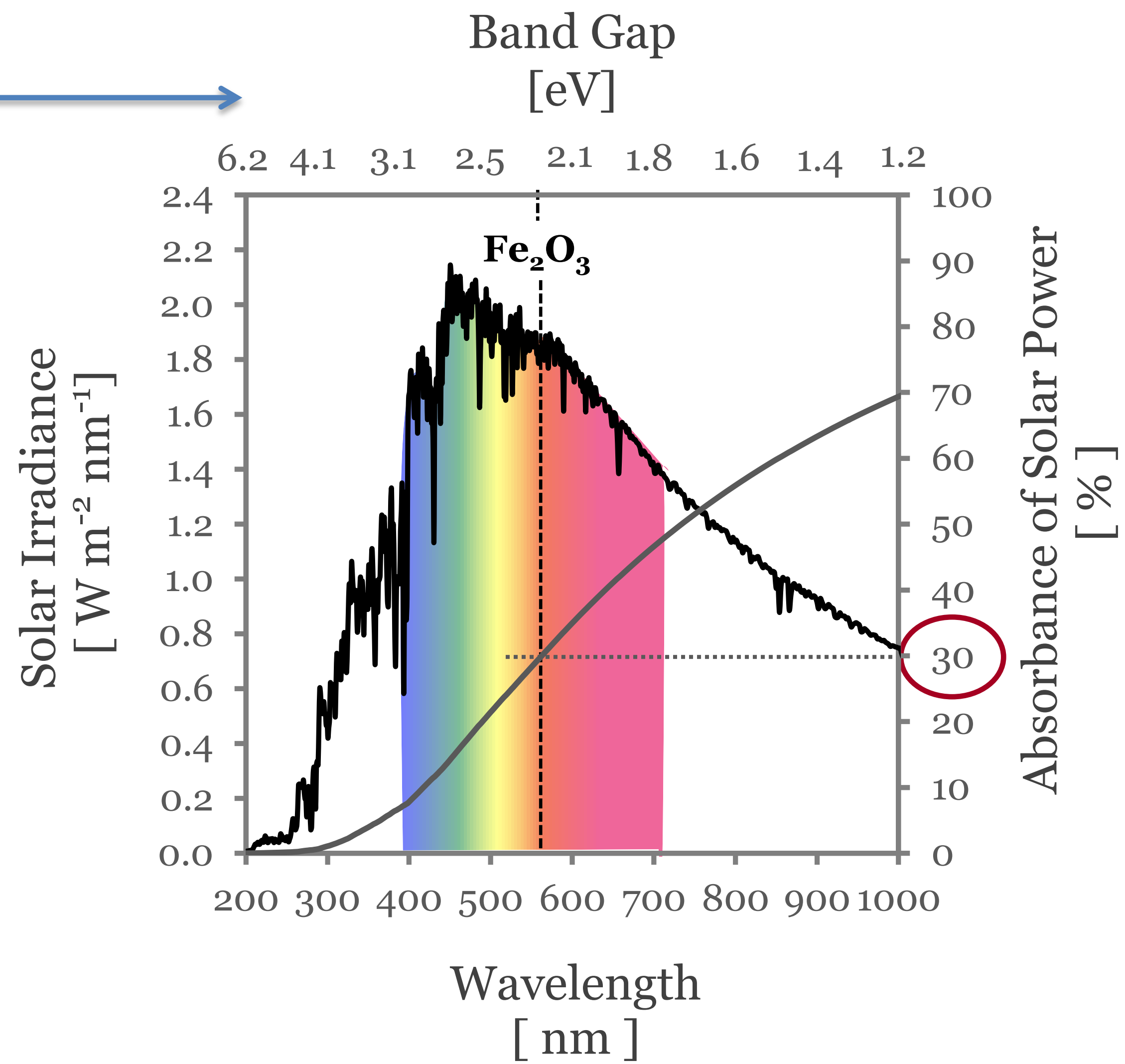

Pros and Cons of Hematite as a Photoanode

Suitability of Fe_2O_3:

- ✓ Absorption spectrum well matched to solar spectrum
- ✓ Easily fabricated on a large scale at low cost
- ✓ Stable to decomposition by ***e***⁻ and ***h***⁺ over wide potential range
- ✓ Valence band energy below that for decomposition of H_2O to O_2

Limitations of Fe_2O_3:

- × Conduction band energy below decomposition potential for H_2O to H_2
- × Stable only in neutral / alkaline pH

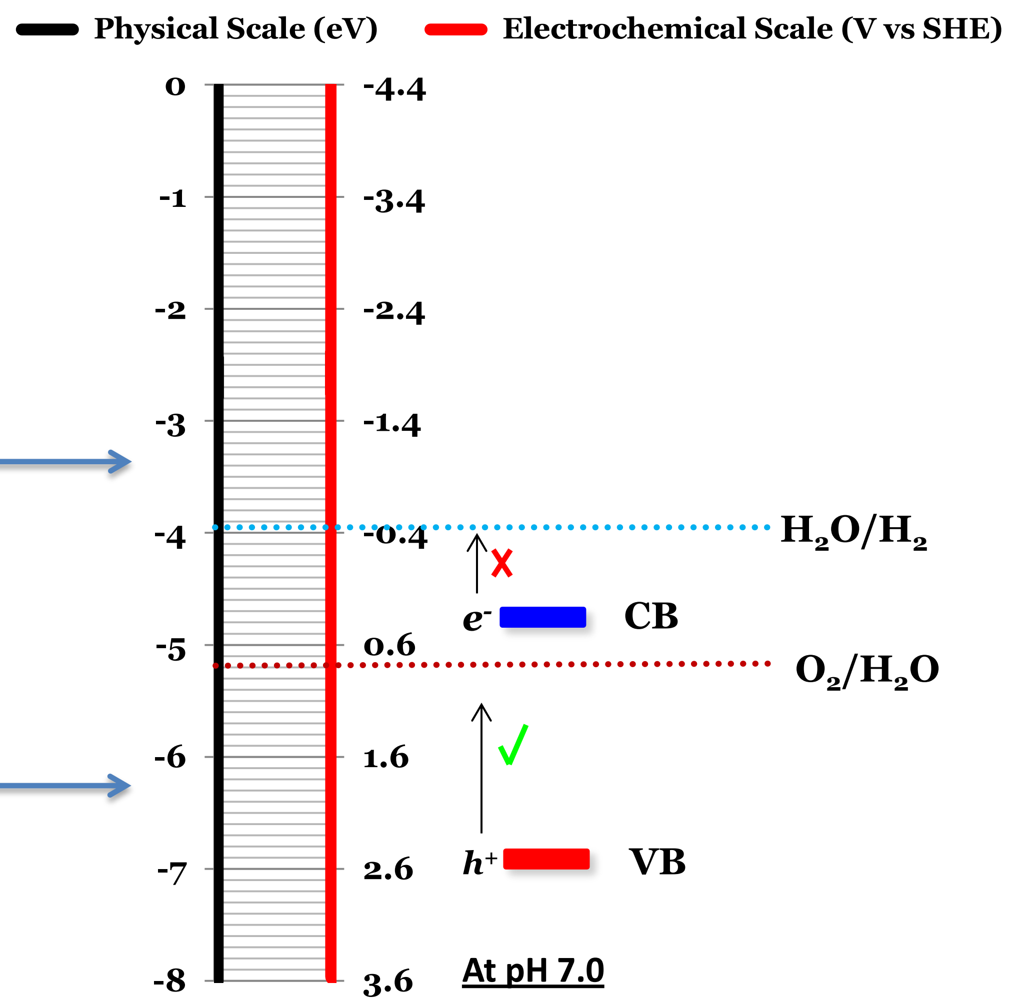

Hematite Photoanode Production

Fabrication of Fe_2O_3 and Sn^{IV}-Fe_2O_3 by Spray Pyrolysis

1. Compressed Air
2. Precursor reservoir
3. Syringe pump
4. Quartz nebuliser
5. CNC machine
6. Substrate
7. Clamping block
8. Hotplate

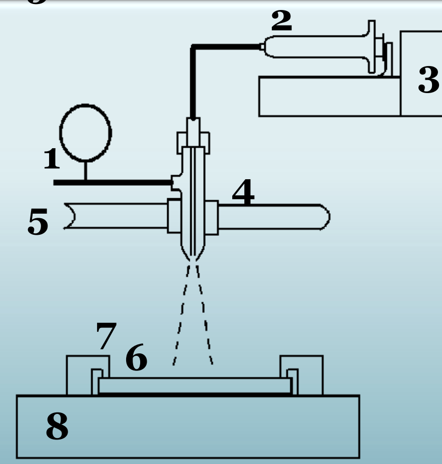

Fe_2O_3 coating produced by nebulising $Fe^{III}Cl_3$ and $Sn^{IV}Cl_4$ in solvent onto heated FTO glass

The Electrode

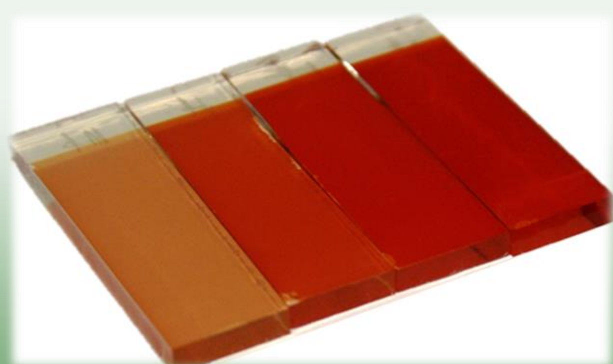

Photographic image

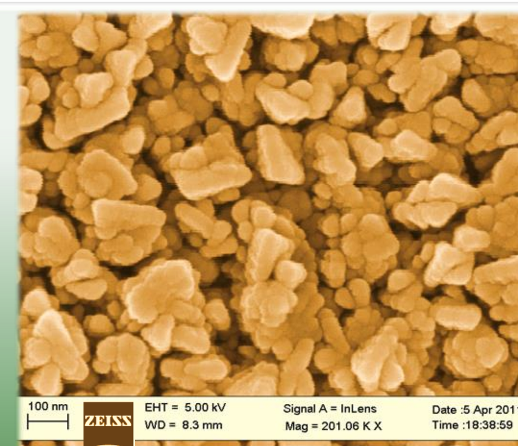

SEM image

Hematite Photo-Response in Steady State

Effect of Potential (applied at 1mV s⁻¹) and White Light Illumination (49 W m⁻² Xe) on
ca. 40 nm thick films on FTO | 1 M NaOH (pH 13.7)

Illuminated area
≈ 0.15 cm²

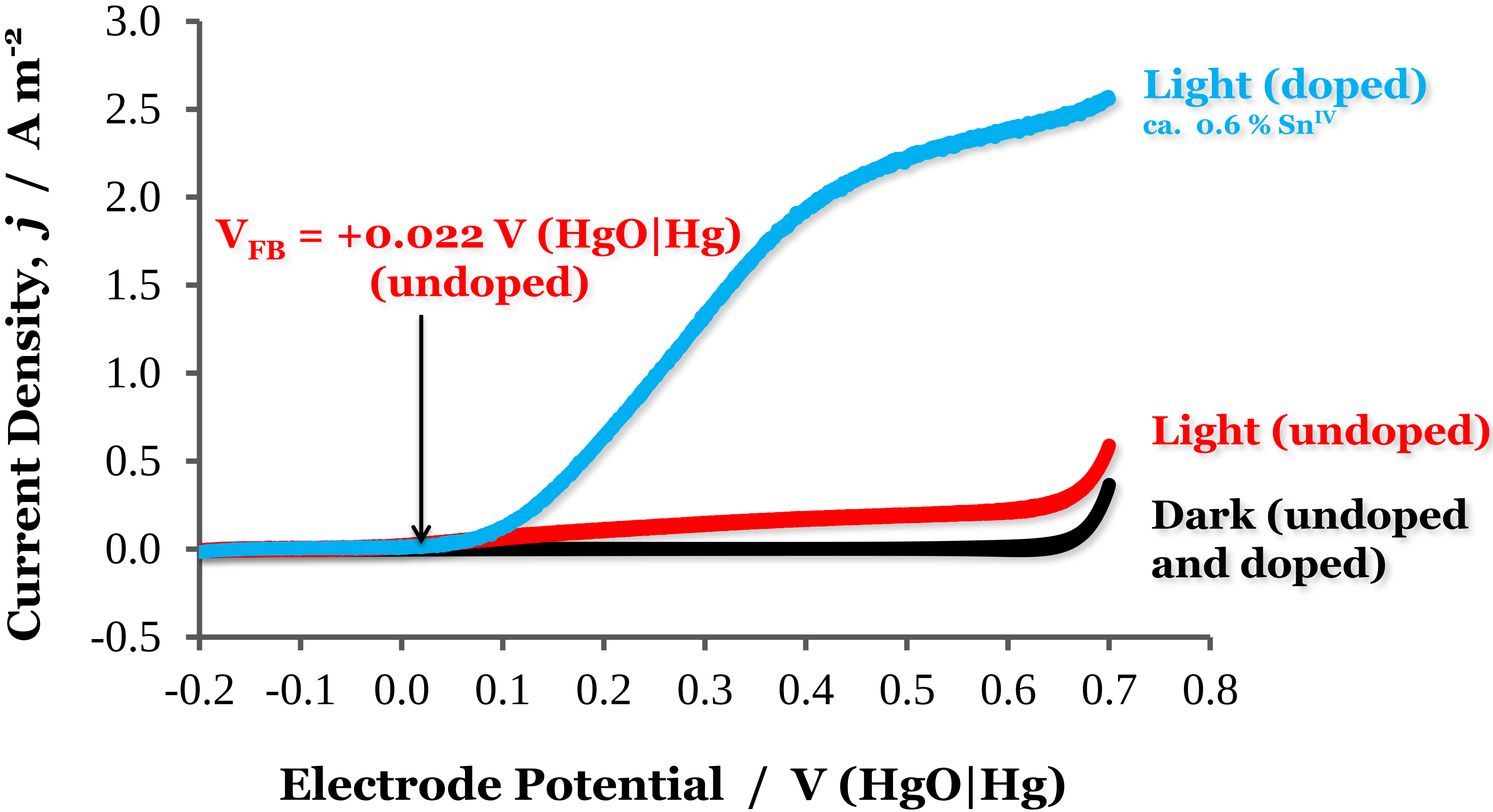

Flat Band and Charge Carrier Determination

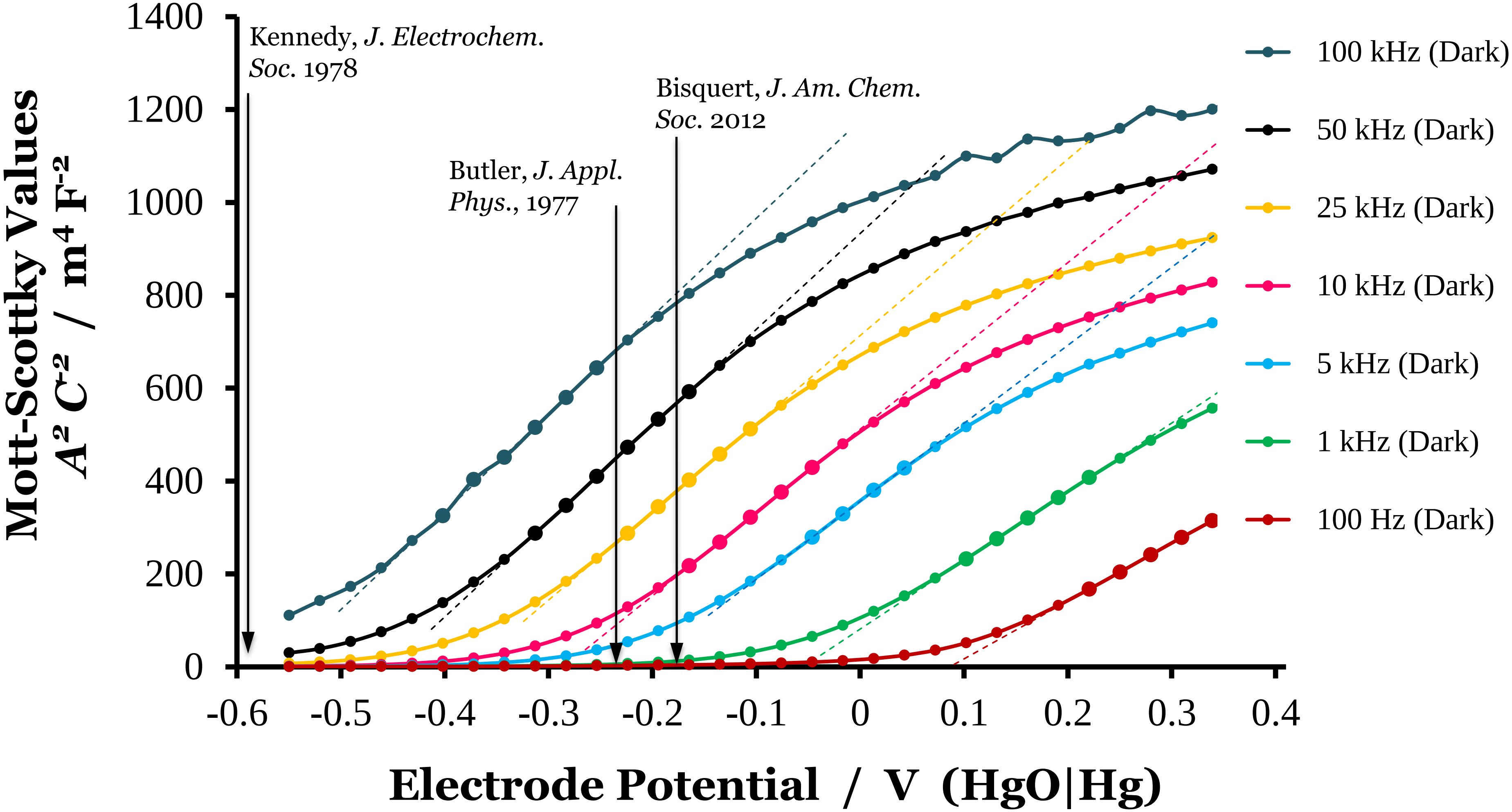

$$V_{FB} = V_{\text{x-intercept}} - \frac{k_B T}{e_0}$$

Evaluation of the Flat Band Potential from j_2 vs V

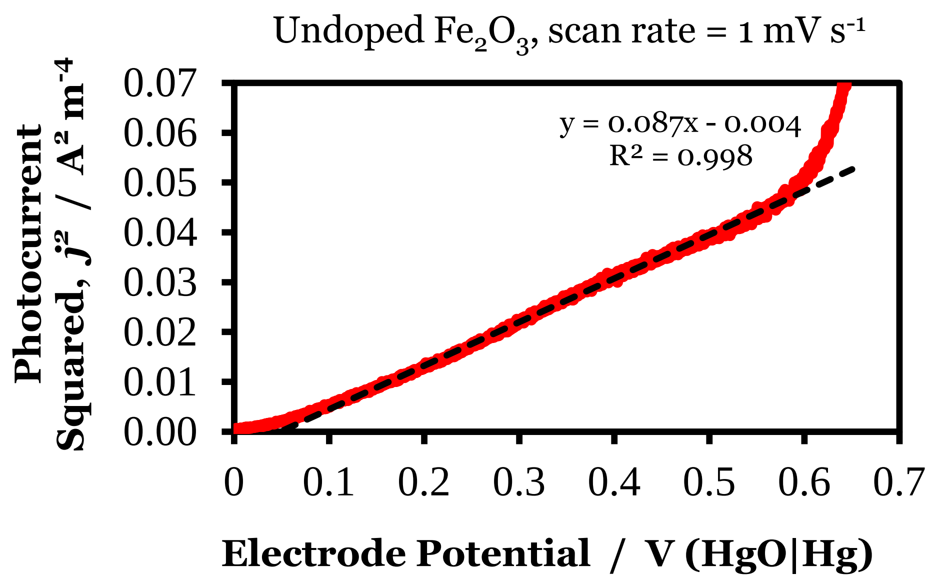

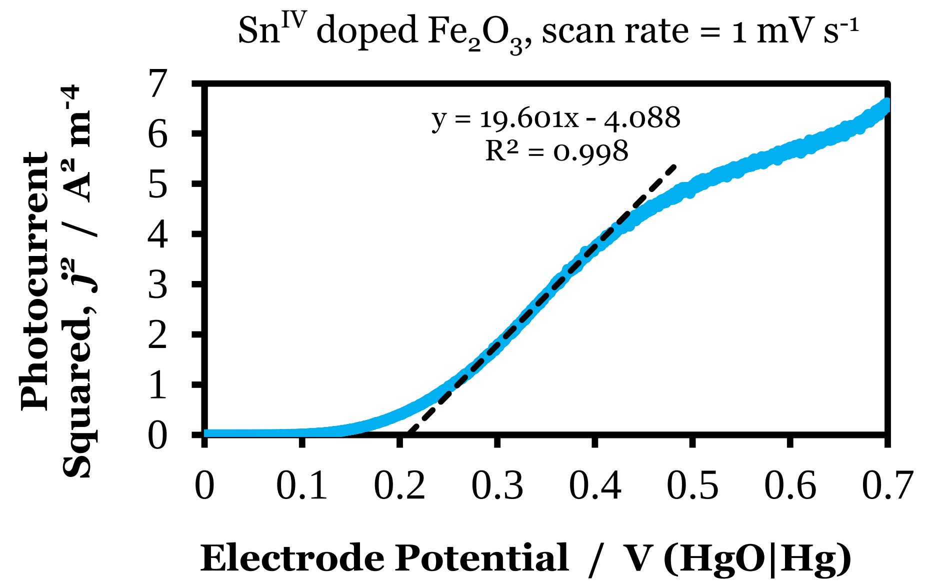

$$V_{FB} = V_{\text{x-intercept}}$$

Material	V_{FB} (HgO|Hg) / V	*pH of zero charge*
Undoped Fe_2O_3	+0.02	6.7 *
Sn^{IV} doped Fe_2O_3	+0.18	< 6.7 (?)

* Watanabe H., Seto J. (1986) *B. Chem. Soc. Jpn.* **59**, 2683

Verification of the Solid|Liquid Energetic Alignment

$$\Delta V_H = \frac{2.3RT}{F}\left[\{pH(pzc)-pH\} - \log\left\{\frac{[Fe-O^-]}{[Fe-OH_2^+]}\right\}^{\frac{1}{2}}\right]$$

For Fe_2O_3 in alkaline solution

$$pH >> pH(pzc) \text{ and } \frac{[Fe-O^-]}{[Fe-OH_2^+]} >> 1$$

$$E_A + \Delta E = -(V_{F\,(measured)} - V_H + 4.44 + E^0(RE\ vs\ SHE))$$

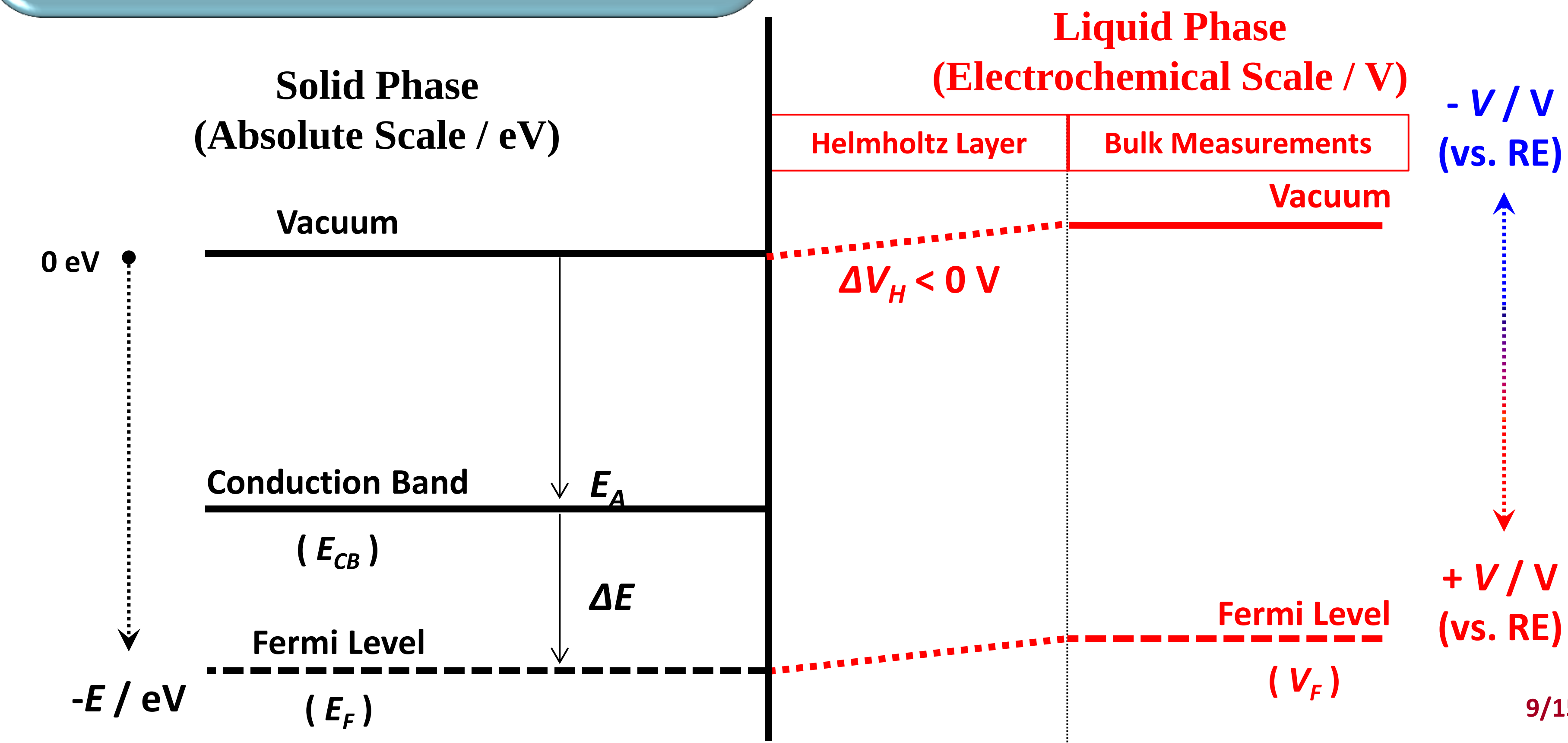

Modelling the Hematite | Liquid Interface

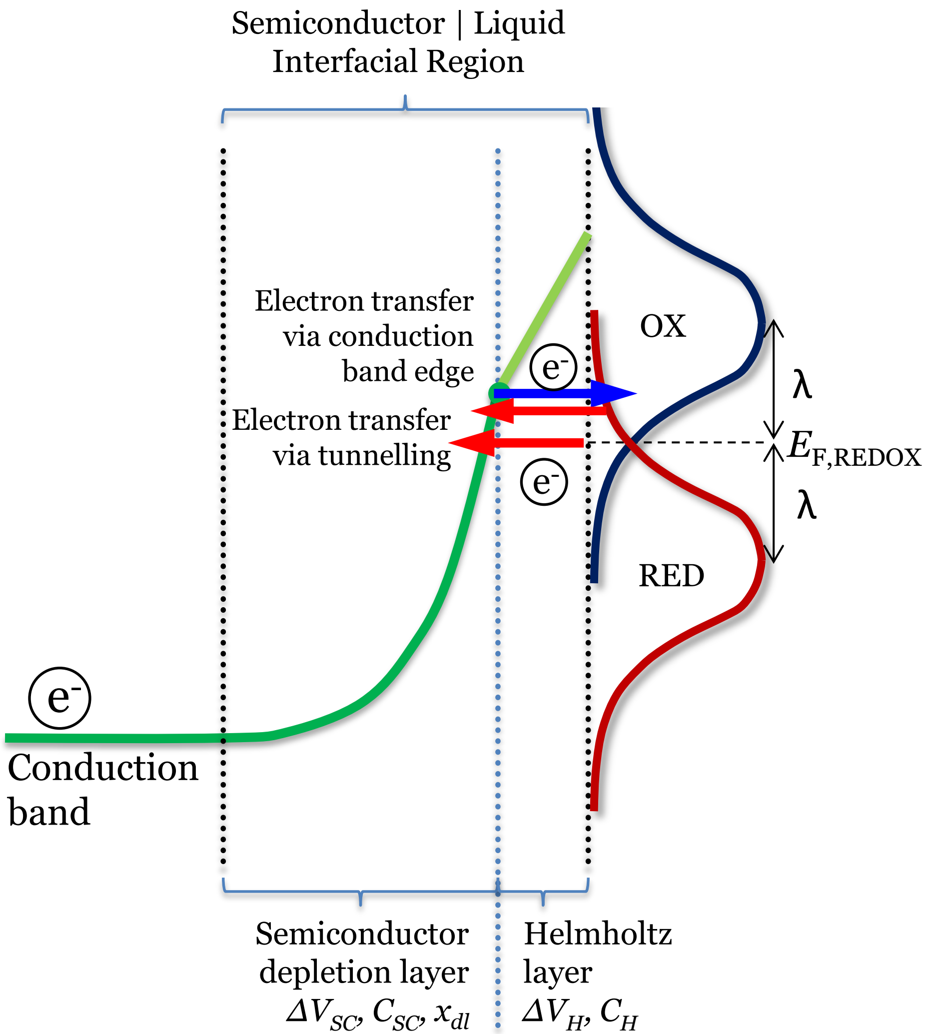

Constructing an Interfacial Model

- Distribution of applied bias $$\Delta V_{Interface} = \Delta V_{SC} + \Delta V_H$$
- Potential drop across the Helmholtz layer $$\Delta V_H = \Delta V_{H,0} + \frac{Q_{SC}}{C_H}$$
- Electric charge in semi-conductor depletion layer $$Q_{SC} = \left(2\varepsilon\varepsilon_r e_0 N_D\right)^{\frac{1}{2}}\left(\Delta E_{SC} - \frac{k_B T}{e_0}\right)^{\frac{1}{2}}$$
- Total interfacial capacitance $$\frac{1}{C_{Interface}} = \frac{1}{C_{SC}} + \frac{1}{C_H}$$
- Semiconductor capacitance $$C_{SC} = \left(\frac{2}{\varepsilon_0\varepsilon_r e_0 N_D}\left(V_{F,SC} - V_{FB} - \frac{k_B T}{e_0}\right)\right)^{-\frac{1}{2}}$$
- Depletion layer thickness $$x_{dl} = 2L_D\left(\frac{\varepsilon_0 \Delta V_{SC}}{k_B T} - 1\right)^{0.5}$$
- Tunnelling distance and probability

$$x_{tunnelling} = 2\left(\frac{\varepsilon\varepsilon_0}{2e_0 n_{CB}}\right)^{\frac{1}{2}}\left[\left(E_{CB}^{Bulk} - E_{CB}^{Surface}\right)^{\frac{1}{2}} - \left(E_{CB}^{Bulk} - E_{rev,O_2/H_2O}\right)^{\frac{1}{2}}\right] + x_{dl}$$

$$T(e_0\phi_{CB}, E_D) = \exp\left[-K\left(\sqrt{e_0\phi_{CB} \times E_D} - (e_0\phi_{CB} - E_D)\ln\left\{\frac{\sqrt{e_0\phi_{CB}} - \sqrt{E_D}}{\sqrt{e_0\phi_{CB} - E_D}}\right\}\right)\right]$$

$$K = \frac{4\pi e_0}{h}\sqrt{\frac{4m_e^*\varepsilon_0\varepsilon_r}{N_D e_0^2}} \quad ; \quad E_D = E_{CB}^{Surface} - E_{REDOX}$$

Model Predictions for Interfacial Behaviour

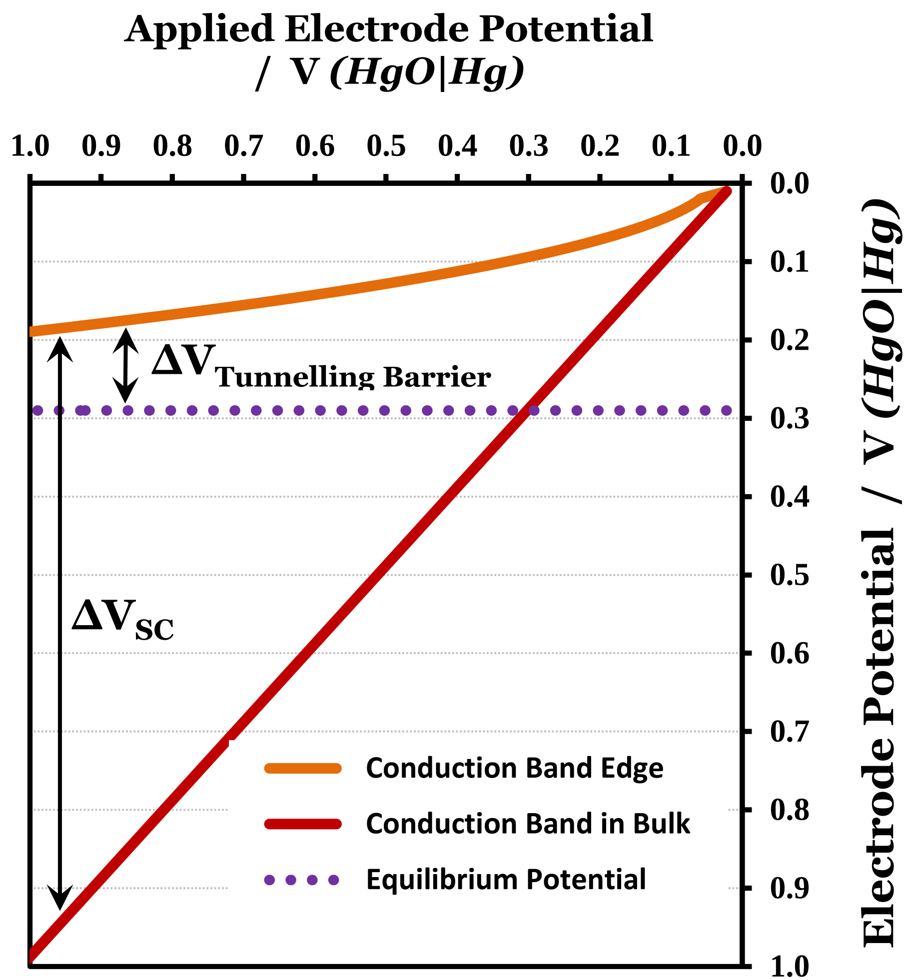

$$\Delta V_{Tunnelling} = V_{Rev} - V_{CB}^{Surface}$$

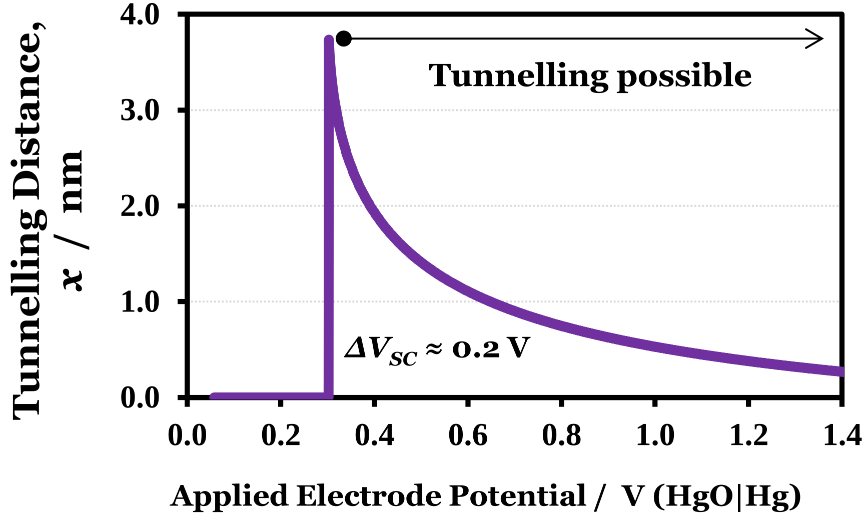

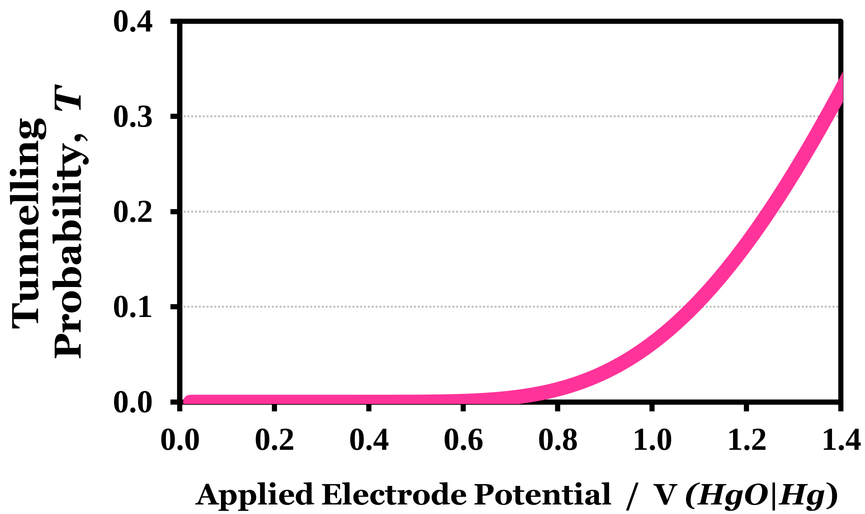

Interfacial Charge Transfer Prediction

j_{Total} = Anodic & Cathodic currents through CB edge + Anodic tunnelling current into CB

$$j = \frac{j_{T,0}\exp\left\{\frac{\alpha F}{RT}(E_F - E_{redox})\right\}T(x(E_F)) + C\left(OH^-\right)N_{CB}\left(\frac{k_BT}{\lambda\pi}\right)^{\frac{1}{2}}\exp\left\{-\frac{e_0^2(E_{CB}^{Edge} - E_{redox} + \lambda)^2}{2\lambda k_BT}\right\}}{\left(1+\frac{j_{T,0}\exp\left\{\frac{\alpha F}{RT}(E_F - E_{redox})\right\}T(E_F) + C\left(OH^-\right)N_{CB}\left(\frac{k_BT}{\lambda\pi}\right)^{\frac{1}{2}}\exp\left\{-\frac{e_0^2(E_{CB}^{Edge} - E_{redox} + \lambda)^2}{2\lambda k_BT}\right\}}{4Fk_{m,OH^-}\left[OH^-\right]}\right)} - \frac{C\left(O_2(aq)\right)N_{CB}\exp\left\{-\frac{e_0}{k_BT}\left(E_{CB}^{Edge} - E_F\right)\right\}\left(\frac{k_BT}{\lambda\pi}\right)^{\frac{1}{2}}\exp\left\{-\frac{e_0^2(E_{CB}^{Edge} - E_{redox} - \lambda)^2}{2\lambda k_BT}\right\}\exp\left\{\frac{(1-\alpha)F}{RT}(E_F - E_{redox})\right\}}{\left(1+\frac{C\left(O_2(aq)\right)N_{CB}\exp\left\{-\frac{e_0}{k_BT}\left(E_{CB}^{Edge} - E_F\right)\right\}\left(\frac{k_BT}{\lambda\pi}\right)^{\frac{1}{2}}\exp\left\{-\frac{e_0^2(E_{CB}^{Edge} - E_{redox} - \lambda)^2}{2\lambda k_BT}\right\}\exp\left\{\frac{(1-\alpha)F}{RT}(E_F - E_{redox})\right\}}{4Fk_{m,O_2}\left[O_2(aq)\right]}\right)}$$

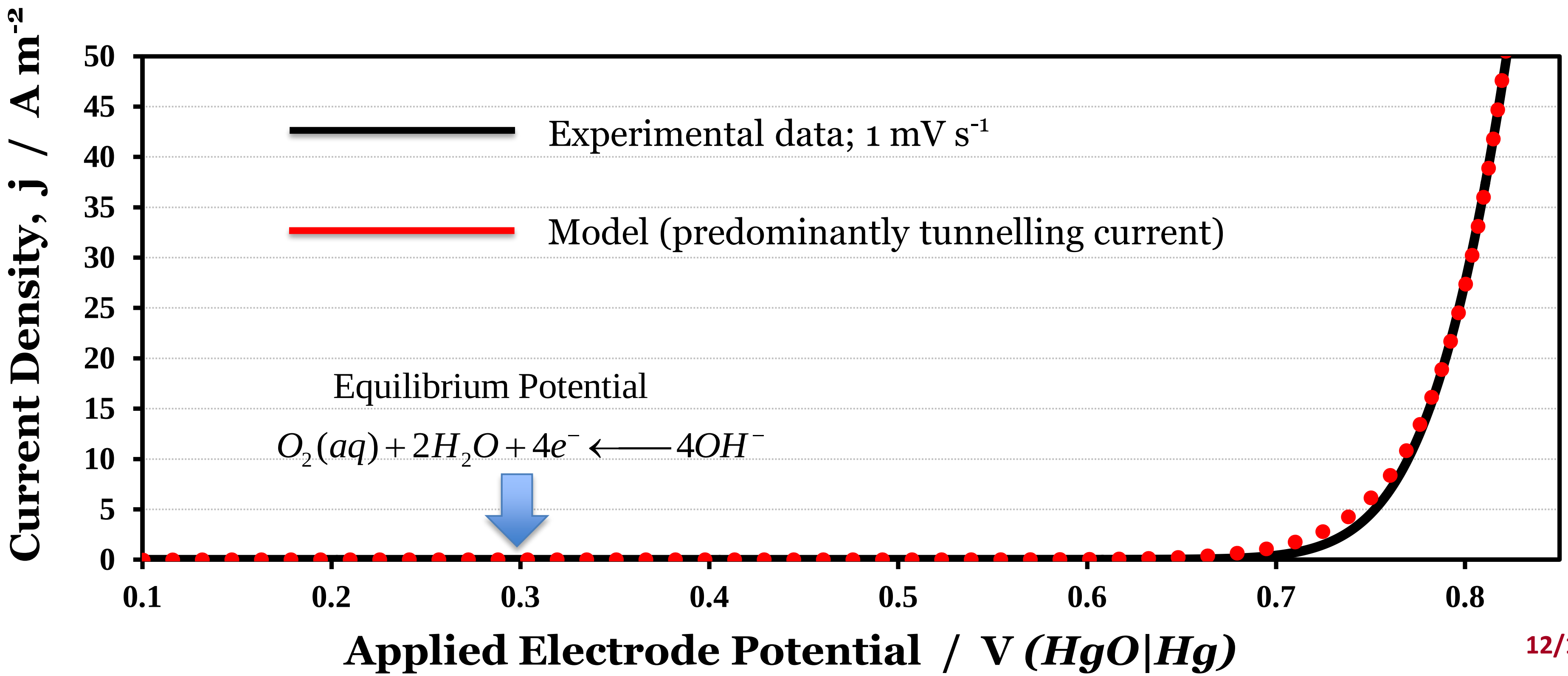

Frequency Dependence of Charge Carrier Concentration

The charge carrier densities are calculated from the slopes of Mott-Schottky plots, obtained at higher frequencies

$$N_D = \frac{2}{\varepsilon_0 \varepsilon_r e_0} \frac{d\left(C^2 A^{-2}\right)}{dV}$$

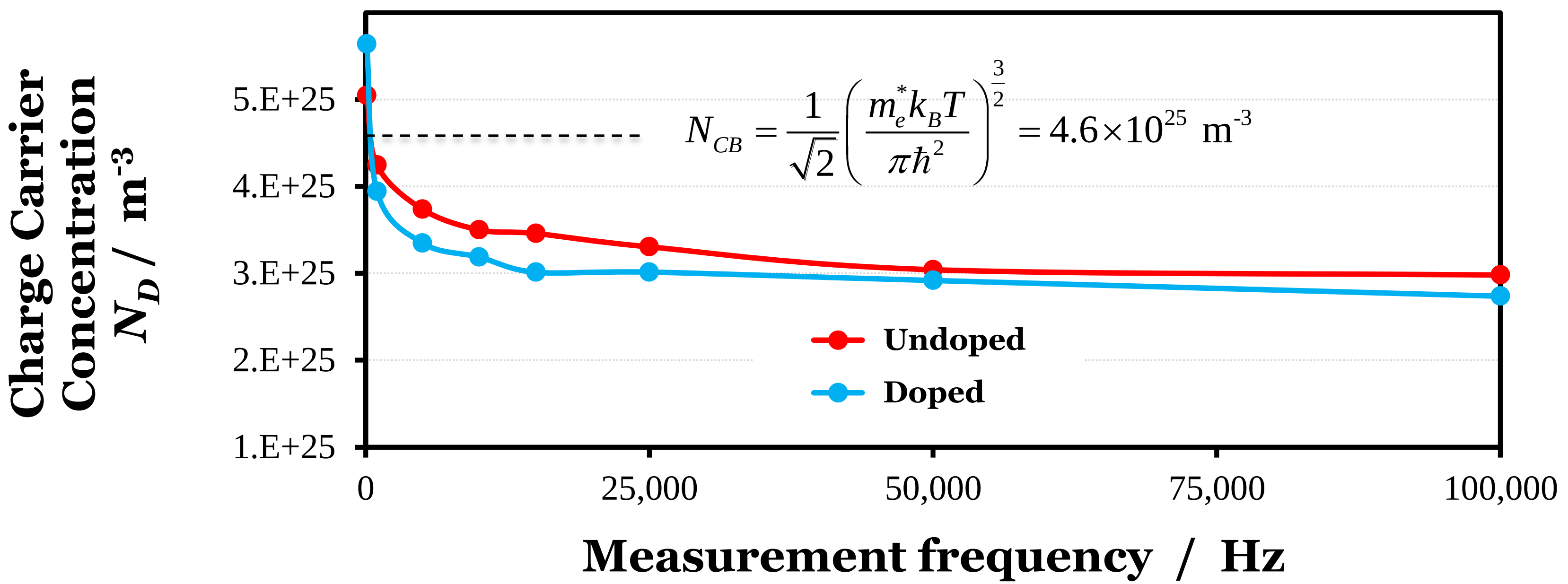

Material	N_D / m^{-3}
Undoped Fe_2O_3	2.80×10^{25}
Sn^{IV} doped Fe_2O_3	2.75×10^{25}

$m_e^* = 1.5 m_e^0$, Peng H., Lany S. (2012) *Phys. Rev. B* **85**, 201202-1

Effect of Dopant of Recombination Kinetics

Analysis of typical Nyquist plots obtained under illumination

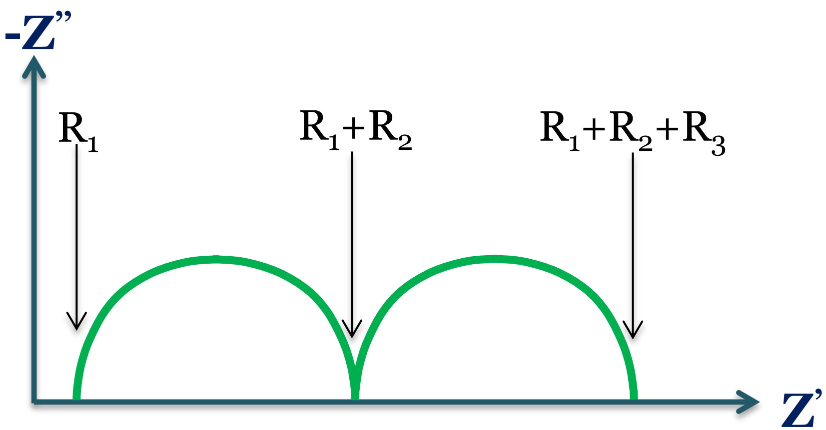

$$\frac{k_{recombination}}{k_{transfer}} = \frac{(R_3 - R_1)}{(R_2 - R_1)} - 1$$

K.G. Upul Wijayantha, S. Saremi-Yarahmadi and L.M. Peter, *Phys. Chem. Chem. Phys.* **13**, 2011, 5264

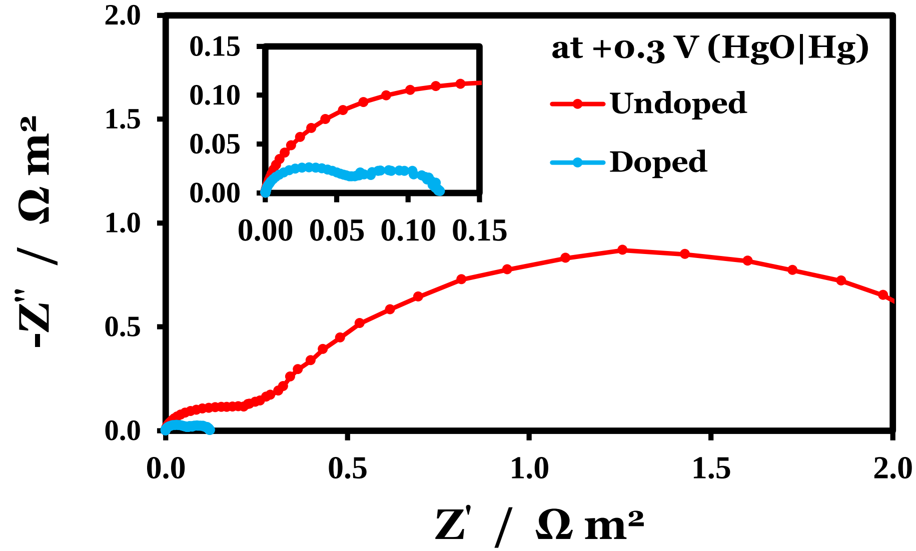

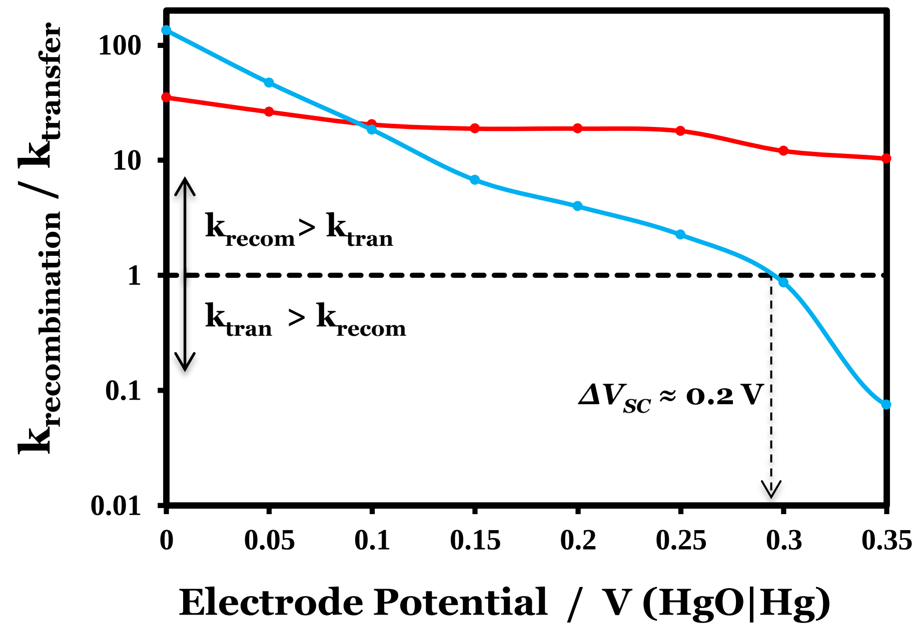

Conclusions

- We have obtained a reasonably good understanding of interfacial behaviour of undoped Fe_2O_3 films in steady state
  - Photocurrent onset potential cannot be shifted further left as limited by flat band potential, obtained from j^2 vs. V plots
  - To maximise the photocurrent, surface area should be increased and recombination rate minimised

- The influence of dopants must be better understood, particularly their effect on recombination rate
- The pH of zero charge must be experimentally determined for each film in order to improve model accuracy

END

Interfacial Characteristics of the Undoped Fe_2O_3

$$E_A + (E_{CB} - E_F) \quad = \quad -\left(V_{F\,(measured)} - \Delta V_H + 4.44 + E^0(RE\ vs\ SHE) \right)$$

Quantity	Value	Unit	Reference
On the absolute scale			
E_A	-4.72	eV	Butler M.A., Ginley D.S., Eibschutz M. (1977) *J. Appl. Phys.* 48, 3070
ΔE	-0.013	eV	Calculated using the charge carrier density, n_{CB}, obtained from Mott-Schottky plots
On the electrochemical scale			
V_{FB} *(measured)*	+ 0.022	V (HgO|Hg)	Determined from the intercept of $(j_{photocurrent})^2$ with the x-axis
ΔV_H	-0.15	V	Calculated as the only unknown in the energy-potential balance
$[Fe\text{-}O^-] / [Fe\text{-}OH_2^+]$ *(at surface)*	8.38×10^8	1	
For the conversion between the two scales			
$E^o(RE) = E^o(HgO\|Hg)$	+0.12	V (SHE)	Experimentally measured
$E^o(SHE)$	0	V (SHE)	Standard value

Electrochemical Impedance of Hematite in the Dark

Circuit representation of the interfacial charge transfer